Technical Report 1300
July 1989

Low-Altitude Millimeter-Wave Propagation in the Evaporation Duct

K. D. Anderson

DISCLAIMER NOTICE

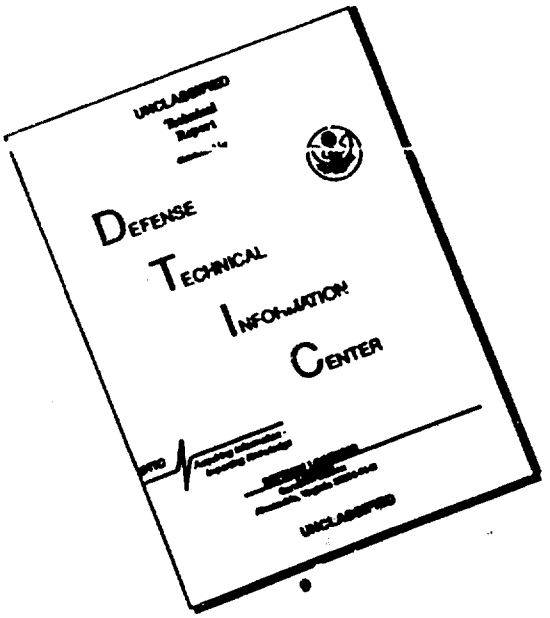

THIS DOCUMENT IS BEST QUALITY AVAILABLE. THE COPY FURNISHED TO DTIC CONTAINED A SIGNIFICANT NUMBER OF PAGES WHICH DO NOT REPRODUCE LEGIBLY.

REPORT DOCUMENTATION PAGE

1a. REPORT SECURITY CLASSIFICATION UNCLASSIFIED	1b. RESTRICTIVE MARKINGS
2a. SECURITY CLASSIFICATION AUTHORITY	3. DISTRIBUTION/AVAILABILITY OF REPORT Approved for public release; distribution is unlimited.
2b. DECLASSIFICATION/DOWNGRADING SCHEDULE	
4. PERFORMING ORGANIZATION REPORT NUMBER(S) NOSC TR 1300	5. MONITORING ORGANIZATION REPORT NUMBER(S)
6a. NAME OF PERFORMING ORGANIZATION Naval Ocean Systems Center 6b. OFFICE SYMBOL (if applicable) Code 543	7a. NAME OF MONITORING ORGANIZATION
6c. ADDRESS (City, State and ZIP Code) San Diego, California 92152-5000	7b. ADDRESS (City, State and ZIP Code)
8a. NAME OF FUNDING/SPONSORING ORGANIZATION OCNR 8b. OFFICE SYMBOL (if applicable)	9. PROCUREMENT INSTRUMENT IDENTIFICATION NUMBER
8c. ADDRESS (City, State and ZIP Code) Arlington, VA 22217-5000	10. SOURCE OF FUNDING NUMBERS PROGRAM ELEMENT NO.: 0602435N PROJECT NO.: RA35G80 TASK NO.: N01A AGENCY ACCESSION NO.: DN888 715

11. TITLE (include Security Classification)

LOW-ALTITUDE MILLIMETER-WAVE PROPAGATION IN THE EVAPORATION DUCT

12. PERSONAL AUTHOR(S)

K. D. Anderson

13a. TYPE OF REPORT	13b. TIME COVERED	14. DATE OF REPORT (Year, Month, Day)	15. PAGE COUNT
Final	FROM Oct 1984 TO Jul 1989	July 1989	34

16. SUPPLEMENTARY NOTATION

17. COSATI CODES			18. SUBJECT TERMS (Continue on reverse if necessary and identify by block number)
FIELD	GROUP	SUB-GROUP	
			evaporation duct radio propagation numerical modeling millimeter-wave communication over-the-horizon signal propagation

19. ABSTRACT (Continue on reverse if necessary and identify by block number)

One-way, low-altitude radio propagation measurements at 94 GHz and simultaneous surface meteorological measurements were made on a 40.6-km over-the-horizon, over-water path along the southern California coast to assess the effects of the evaporation duct on signal propagation. More than 2000 hours of received signal power were recorded in eight measurement periods from July 1986 through July 1987. The average received power was 63 dB greater than expected for propagation in a nonducting, or standard, atmosphere; 90% of the measurements were at least 55 dB greater than the standard atmosphere.

Predictions of transmission loss based on the observed surface meteorology compared favorably to the measured transmission loss; on the average, the predictions underestimated the transmission loss by 10 dB. The reliability and reasonable accuracy of the model provided a strong justification for utilizing the technique to assess millimeter-wave communication and radar systems operating in many, if not all, ocean regions.

20. DISTRIBUTION/AVAILABILITY OF ABSTRACT	21. ABSTRACT SECURITY CLASSIFICATION	
☐ UNCLASSIFIED/UNLIMITED ☒ SAME AS RPT ☐ DTIC USERS	UNCLASSIFIED	
22a. NAME OF RESPONSIBLE INDIVIDUAL K. D. Anderson	22b. TELEPHONE (include Area Code) (619) 553-1420	22c. OFFICE SYMBOL Code 543

DD FORM 1473, 84 JAN

83 APR EDITION MAY BE USED UNTIL EXHAUSTED
ALL OTHER EDITIONS ARE OBSOLETE

EXECUTIVE SUMMARY

OBJECTIVE

The Naval Ocean Systems Center undertook to assess the effects of the evaporation duct on low-altitude over-the-horizon radio propagation at millimeter wavelengths.

RESULTS

The evaporation duct strongly influences beyond-horizon propagation at millimeter wavelengths. Measurements made at a 3-mm wavelength (94 GHz) on an over-the-horizon, over-water path show that there is more than 60 dB available at the receiver than expected if standard (4/3 earth) propagation models were used. Results from numerical modeling of both the meteorological and propagation characteristics of the path reasonably agree with the observations.

RECOMMENDATIONS

The accuracy of the propagation model provides a strong justification for using it to assess the propagation characteristics of millimeter-wave communication and radar systems operating in many, if not all, ocean regions.

CONTENTS

TABLES

ILLUSTRATIONS

INTRODUCTION

Millimeter-wave systems are attractive because of their small antenna aperture and because of their ability to penetrate a slightly opaque atmosphere (haze, smoke). At longer wavelengths, aperture size can be cumbersome, whereas at shorter wavelengths, the ability to penetrate an opaque atmosphere can be lost. Although the advantages are well known, terrestrial millimeter-wave systems normally operate over short ranges—typically within line of sight—because of propagation limitations imposed by the atmosphere.[1,2]

For low-altitude, over-water applications, the evaporation duct has been shown to be a reliable propagation phenomenon that can dramatically increase beyond-the-horizon signal levels for frequencies greater than 2 GHz.[3-6] Although the highest frequency reported in previous work is 35 GHz, the results show that the magnitude of signal enhancement (referenced to diffraction) increases with increasing frequency. An analysis of measurements in the Aegean Sea shows that the median received signal power on a 35-km path is 2, 15, 27, and 30 dB above diffraction for frequencies of 1, 3, 9.6, and 18 GHz, respectively.[5] The received signal power at 35 GHz on this path is consistently 30 to 45 dB above diffraction.[5]

In this report, the effects of evaporation ducting on over-the-horizon signal propagation at 94 GHz are presented. Results from more than 2000 hours of RF measurements made on a 40.6-km path along the southern California coast are analyzed in terms of path loss (equivalent to transmission loss), which is defined as the ratio of transmitted to received power, assuming loss-free isotropic antennas. Numerical propagation modeling results based on measured and climatological surface meteorology are compared to measured path loss. These comparisons are good, and the results strongly support using the propagation model to predict the performance of millimeter-wave systems operating near the surface in all ocean regions.

A brief review of the evaporation duct model and the propagation model used in this analysis precedes a discussion of the experiment and the results.

EVAPORATION DUCT AND PROPAGATION MODELS

The evaporation duct is a nearly permanent propagation mechanism created by a rapid decrease of moisture immediately above the ocean surface. Air adjacent to the surface is saturated with water vapor and rapidly dries out with increasing height until an ambient value of water vapor content is reached, which is dependent on general meteorological conditions. The nearly logarithmic decrease in vapor pressure causes the refractivity gradient to decrease faster than −157 N/km, which is a trapping condition. The height at which dN/dz equals −157 N/km is defined as the evaporation duct height and is a measure of the strength of the duct. Typical duct heights are between a few meters and approximately 30 meters, with a world-average value of 13.6 meters.[7] Because these ducts are vertically thin, strong trapping is infrequently observed for frequencies below 2 GHz.

In practice, boundary-layer theory relates bulk surface meteorological measurements of air temperature, sea temperature, wind speed, and humidity to the vertical profile of refractivity and thus the evaporation duct height. In a thermally neutral atmosphere where the air–sea temperature difference is 0, the modified refractivity profile is given by

$$M(z) = M(0) + 0.125\{z - \delta \cdot \ln[(z + z_0)/z_0]\} \quad (1)$$

where z is height above the ocean, δ is evaporation duct height, and z_0 is a length characterizing boundary roughness. For a thermally nonneutral atmosphere, stability terms are incorporated into Eq. 1 (see Jeske[4]). However, for common departures from neutrality, propagation calculations indicate that a neutral profile is a reasonable approximation, provided that duct height for the neutral profile is calculated from observed meteorology. In this analysis, evaporation duct height is computed from surface observations by using the Jeske model[4,8] as implemented by Hitney[9] with thermal stability modifications suggested by Paulus.[10]

Numerical propagation-modeling techniques have shown good agreement to RF measurement results when single-station surface meteorological observations are available to determine the refractivity-versus-altitude profile of the evaporation duct.[11] In a maritime environment, the assumption of lateral homogeneity (vertical profile of refractivity invariant along the path of propagation) is generally good[11,12] and justifies a waveguide formalism[13–15] approach to the analysis of propagation through the troposphere. Numerical results are derived from a computer program called "MLAYER," which is an enhanced version of the "XWVG" program.[16] MLAYER assumes that the vertical profile of refractivity over the sea can be approximated by an arbitrary number of linear segments and uses an ingenious technique to find all complex modes that propagate with attenuation rates below a specified value.[17] Surface roughness is developed from Kirchhoff–Huygens theory in terms of rms bump height, σ, which is related to wind speed as $\sigma = 0.0051 \cdot u^2$, where u is wind speed (m/s).[18,19]

The determination of the vertical refractivity profile is crucial to the MLAYER calculations. For neutral and stable conditions, the duct height is

$$\delta = \frac{-\Delta\phi *}{1.32 + 0.0867 \cdot R/\Gamma \cdot (0.75 - \Delta\phi)} \quad (2)$$

where $\Delta\phi *$ is the potential refractivity difference between the air and sea surface, R is the bulk Richardson's number, and Γ is an empirical profile coefficient. Equation 2 assumes that bulk parameters are measured at a height of 6 meters and that z_0 is 0.00015 meter. Under neutral conditions, R is zero; hence the potential refractivity difference is $\Delta\phi * = -1.32 \cdot \delta$. The potential refractivity gradient (under neutral and stable conditions) is

$$\frac{\Delta\phi}{\Delta z} = \frac{\Delta\phi *(1.0/z + 0.867 \cdot R/\Gamma)}{10.60 + 0.52 \cdot R/\Gamma} \quad (3)$$

where z is the height above the surface. Again, under strictly neutral conditions, Eq. 3 reduces to $\Delta\phi/z = \Delta\phi */(10.60z)$. The potential refractivity gradient is related to the refractivity gradient as $\Delta\phi/\Delta z \approx \Delta N/\Delta z + 0.032$ and to the modified refractivity gradient as $\Delta\phi/\Delta z \approx \Delta M/\Delta z - 0.125$. From Eq. 2 and 3, the modified refractivity pro-

file was determined for evaporation duct heights from 0 to 20 meters in 2-meter intervals. These profiles are approximations of results obtained by using Eq. 1. This technique, however, allows for the inclusion of thermal stability and has been used in previous studies. The primary reason for using Eq. 2 and 3 over the more direct approach specified in Eq. 1 was to maintain a consistency with prior work.

Once the profiles were established, path-loss calculations were made for five rms bump heights: 0.0 (smooth surface), 0.025, 0.100, 0.250, and 0.500 meters, corresponding to wind speeds of 0.0, 4.3, 8.6, 13.6, and 19.2 knots. Approximately 500 hours of computer time were needed to complete these calculations; most of the computer time was devoted to finding the waveguide modes in the complex plane. Although the computational expenditures were significant, once the modes were found, path loss could be calculated efficiently for almost any path geometry.

For a one-way transmission system, signal power at the receiver is

$$P_r = P_t + G_t - L + G_r + G_a \tag{4}$$

where P_t is power transmitted, L is transmission loss, G_t and G_r are transmitter and receiver antenna gains, and G_a is additional gain measured from the receiver antenna to the point in the receiver where power is measured. Assuming that transmission-line losses and other hardware-related losses are accounted for in P_t and G_a, the loss L can be written as $L = L_m + L_c$, where L_m is loss due to molecular absorption and L_c is loss accounting for all other environmental and geometrical losses. The advantage of treating L as the sum of two independent terms is that L_m then depends on observable air temperature and humidity, whereas L_c depends on the same two observables in addition to sea temperature and wind speed. Of course, both loss terms depend on the geometry of the transmission path; L_m is the product of attenuation rate and path length, and L_c involves a complicated dependency on the refractivity profile, path length, and antenna heights.

Range dependency of absorption-free path loss (L_c) at a frequency of 94 GHz is shown in Fig. 1 for a standard atmosphere, denoted by 0 duct height, and for evaporation duct profiles (neutral stability) corresponding to duct heights of 2, 4, 6, and 8 meters. In this case, transmitter and receiver are 5 and 9.7 meters above a smooth sea surface, and coherent signal propagation (modal phasing included) is assumed. At a range separation of 40 km, L_c for transmission through a standard atmosphere is about 250 dB (assuming a typical 0.7 dB/km molecular absorption attenuation rate, total path loss is about 280 dB). For propagation in an atmosphere represented by a refractivity profile corresponding to an evaporation duct height of 2 meters (a relatively shallow duct), L_c is approximately 184 dB—a "gain" of 66 dB compared to the diffraction reference. With an 8-meter evaporation duct, path loss increases with range at a fairly consistent rate of about 0.2 dB/km beyond 30 km.

Path-loss variation with receiver height is shown in Fig. 2 for a path separation of 40.6 km. The transmitter is located 5 meters above a smooth surface. In a standard atmosphere, path loss for a receiver located 20 meters above the surface is about 230 dB. For this same receiver in an environment of a 2-meter evaporation duct, path loss is about 178 dB—a gain of 52 dB even though both transmitter and receiver are outside the duct.

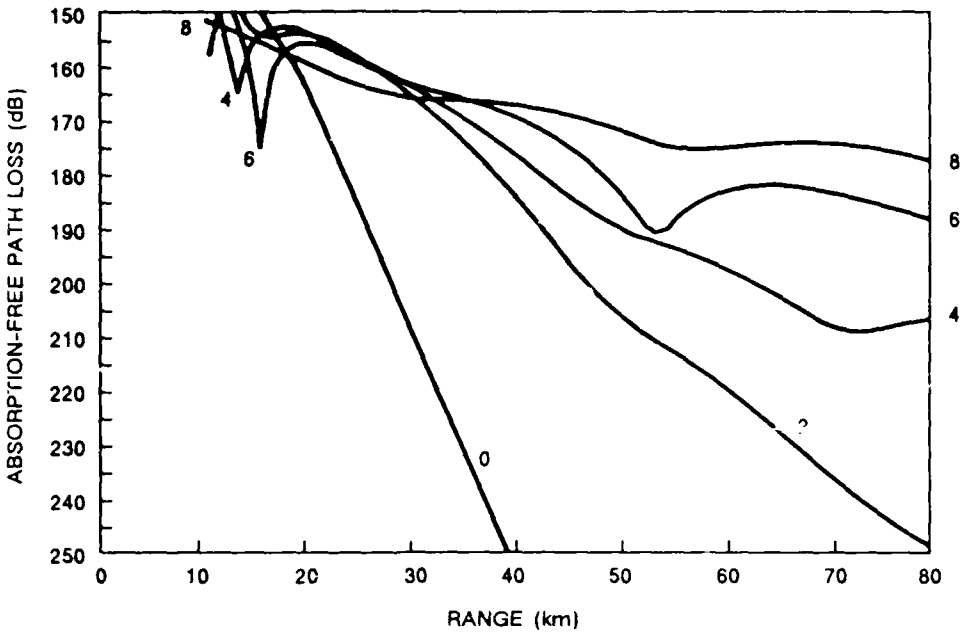

Figure 1. Absorption-free path loss vs range for evaporation duct heights of 0 (standard atmosphere), 2, 4, 6, and 8 meters. Coherent mode summation and smooth surface.

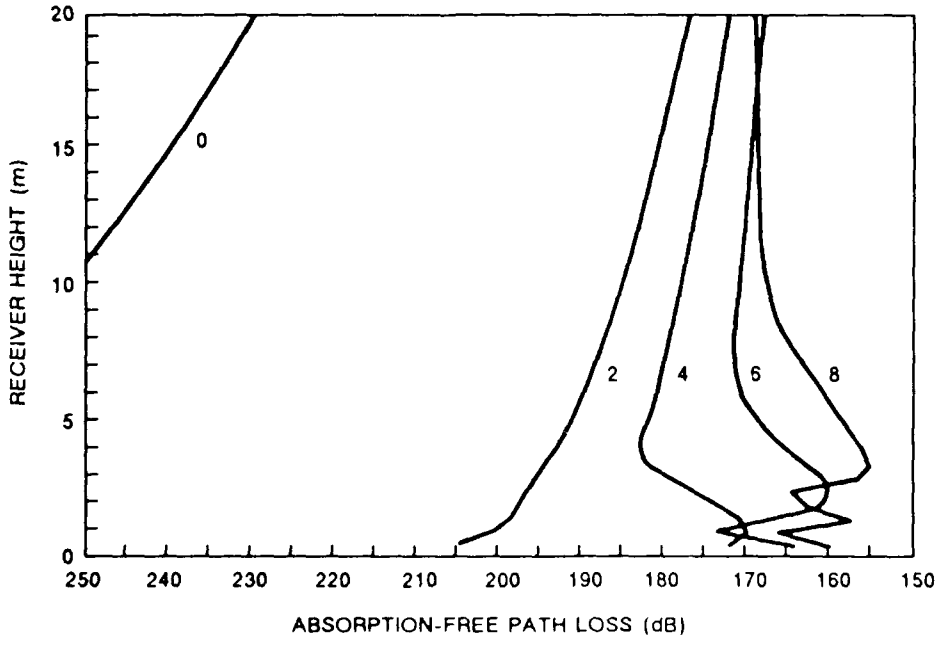

Figure 2. Absorption-free path loss (incoherent) for a transmitter at 5 meters, a range separation of 40.6 km, and a smooth surface. The curves are labeled with the duct height in meters.

Surface roughness effects are shown in Fig. 3 for a transmitter at 5 meters, a receiver at 9.7 meters, and a fixed path separation of 40.6 km. Incoherent signal propagation (r al phase is ignored) is used to represent absorption-free loss, L_c. Higher wind s ds generally increase loss with respect to a smooth surface, except for a standard atmosphere, where the waveguide modes are evanescent. For duct heights above 10 meters, path loss is nearly equal at the two highest wind speeds. Above 16 meters, path loss is nearly equal for wind speeds greater than about 8 knots. In these highly trapped cases, many weakly attenuated modes are found and the aggregate effect is for convergence of the mode sums to a limiting value. At 94 GHz, the limiting value of surface roughness appears to be a bump height of 0.5 meter.

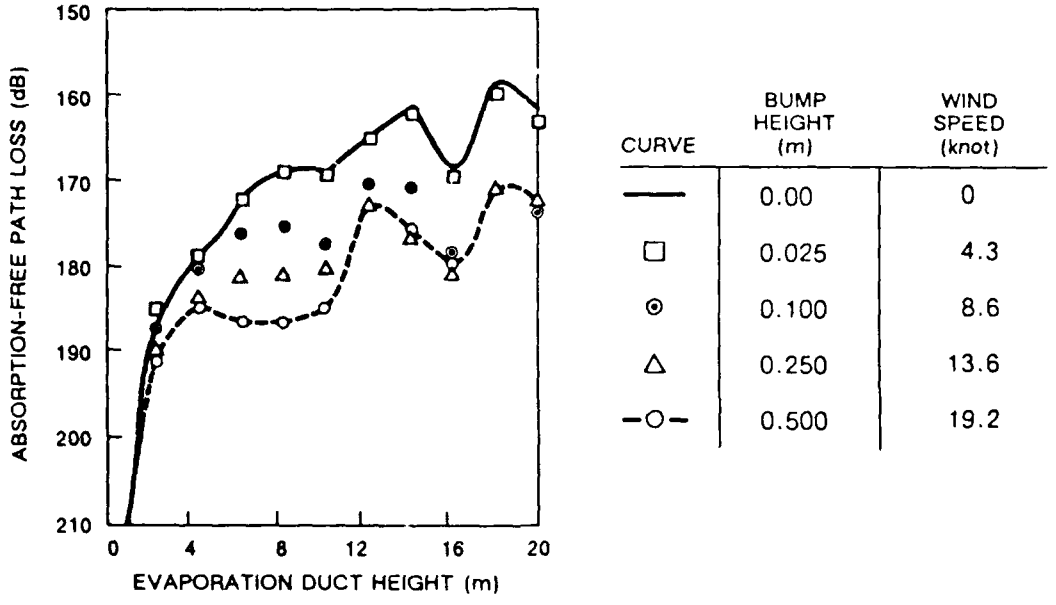

Figure 3. Effects of surface roughness at 94 GHz. Transmitter at 5 meters, receiver at 9.7 meters, and range separation of 40.6 km. The rms bump height, expressing the surface roughness, is derived from Kirchoff-Huygens Theory (see Ament[8] and Phillips[9]).

TEST EQUIPMENT

A 40.6-km transmission path along the Southern California coast was chosen and instr mented for the measurement program. The path i shown in Fig. 4. The transmitter antenna was located 5 meters above mean low water (mlw) at the Del M Boat Basin facility of the U.S. Marine Corps Base at Camp Pendleton, California. This antenna, a horizontally polarized 12-inch-diameter lens with a 0.7-degree beamwidth, was centered along the path at an elevation angle of zero degrees. The horizon is 9.2 km and is shown as a dashed arc in Fig. 4.

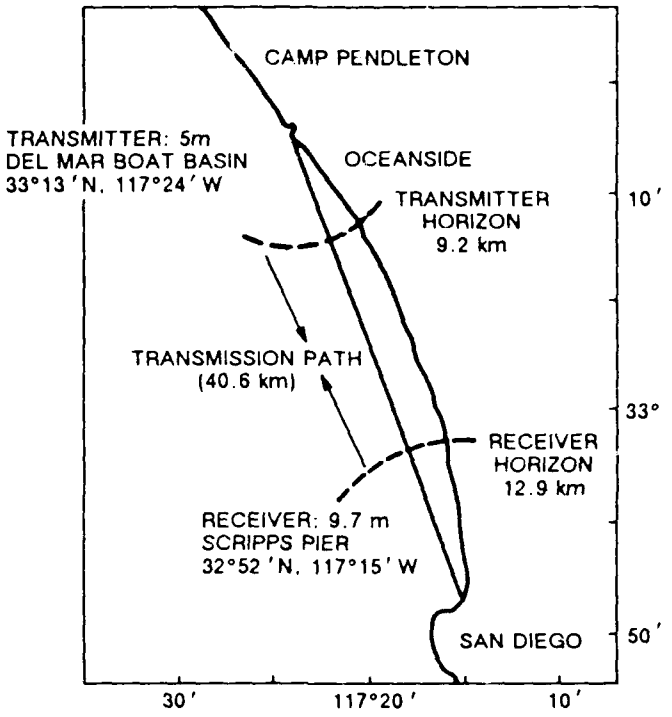

Figure 4. Transmission path used in the measurements.

The receiver site was at the western end of Scripps Pier, located at the University of California at San Diego, California. This pier extended 335 meters from the shore, which, in all but the worst storms, placed the receiver beyond the surf zone. (The pier has since been torn down and replaced by a new structure.) The receiver antenna was located 9.7 meters above mlw (horizon of 12.9 km) and was pointed towards the transmitter with an elevation angle of zero degrees.

A block diagram of transmitter equipment is shown in Fig. 5. An X-band oscillator, phase-locked to a stable 103-MHz crystal source, phase-locked a 94-GHz Gunn diode that injection-locked an IMPATT diode. These components were manufactured by Hughes Electron Dynamics Division to custom specifications and performed admirably. In the original design of the experiment, the injection-locked oscillator (ILO) output was to feed both the antenna and a thermistor power sensor in order to monitor output power during operation. In practice, because of large thermal drifts in the sensor and the power meter, output power was measured manually at the start of, intermittently throughout, and at the end of the measurement period. Observed output power deviations were less than a few tenths of a decibel during the entire year-long measurement program. Phase lock of the 94-GHz ILO was sensed at the first-stage lock-loop intermediate frequency (IF) and recorded by computer.

The receiving system closely resembles the transmitter system and is shown in Fig. 6. A 103-MHz crystal source was offset from the transmitter crystal reference to generate an IF of 59.8 MHz, which was monitored by a spectrum analyzer. Although the controller could adjust analyzer functions to optimize signal detection, the analyzer was typically set for a frequency span of 181.7 kHz, without integration, and with video and resolution bandwidths of 3 kHz. Signal power and frequency were recorded with an effective sample time of 540 ms.

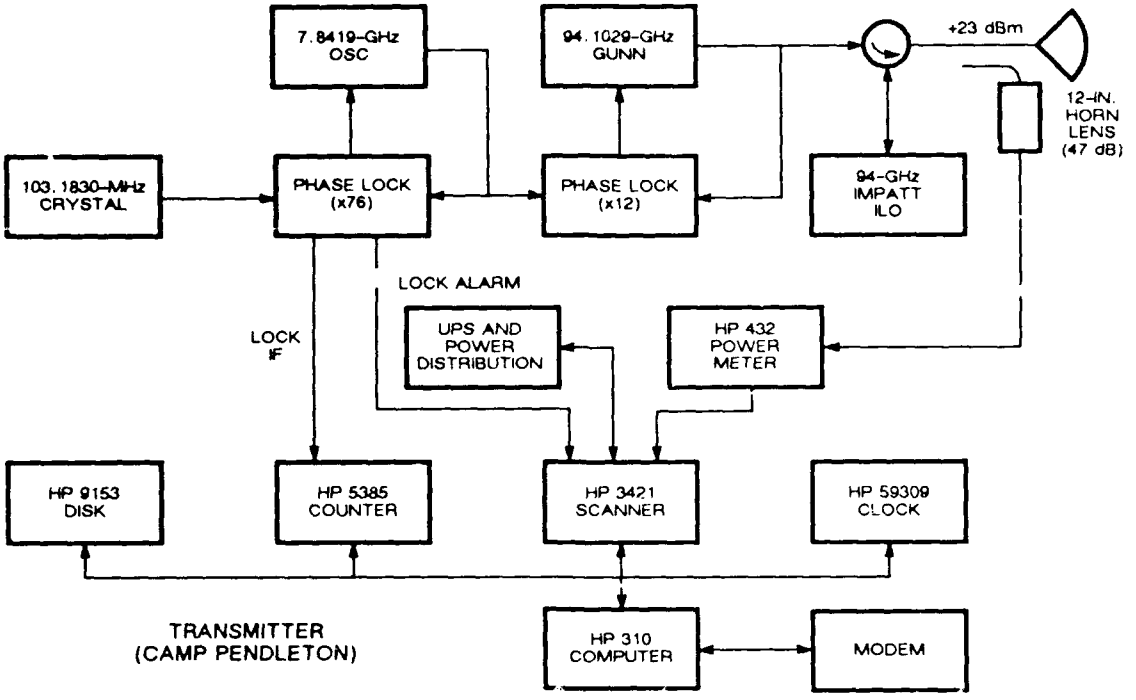

Figure 5. Transmitter system installed at Camp Pendleton, CA.

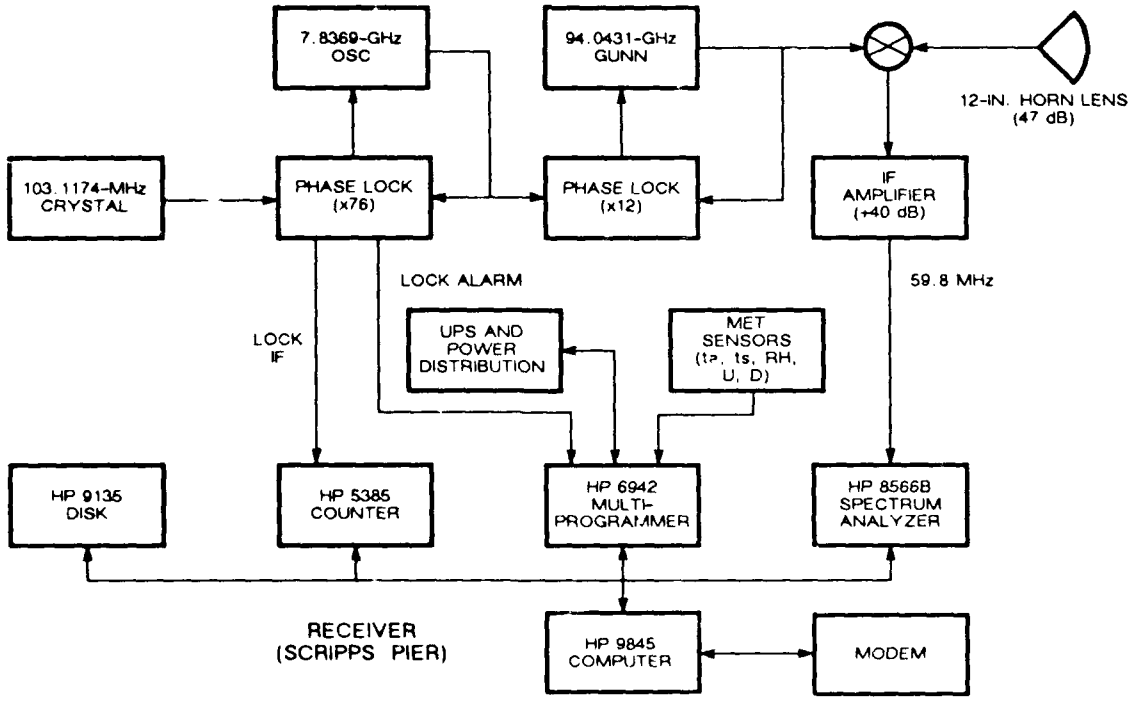

Figure 6. Receiver system installed at Scripps Pier.

System "constants" (power transmitted, antenna gains, and RF-to-IF gain of the receiver) are listed in Table 1. Total path loss is thus related to observed received signal power as $L = 157 - P_r$, which is the sum of the system constants minus the power received (see Eq. 4). The minimum detectable signal power at the analyzer was ≈ -83 dBm, which corresponds to a maximum detectable path loss of ≈ 240 dB (L = 157 – (–83)). Diffraction is about 250 dB for the geometry of the path. Therefore, without evaporation ducting, the signal should be 10 dB below the receiver noise level and should not be detectable. However, the expected gain of about 60 dB through evaporation ducting, less the expected molecular absorption loss of about 30 dB, places the signal at about 220 dB, which is detectable by the receiver.

Table 1. RF system constants.

Component	Value
Transmitter power	23 dBm
Transmitter antenna gain	47 dBi
Receiver antenna gain	47 dBi
Receiver RF-to-IF gain	40 dB

The dynamic range of the analyzer was sufficient to lock onto and track the signal in all conditions, except when there was precipitation along the path, which was rare. A moderate rain shower, uniform along the path, could increase path loss by 100 dB, making any practical reception impossible. As a reference, the basic free-space transmission loss, $(4\pi d/\lambda)^2$, is 164 dB, where d is the range separation and λ is the wavelength.

Air temperature, sea temperature, relative humidity, wind speed, and wind direction were recorded at Scripps Pier in conjunction with the RF measurements. Table 2 describes the surface meteorological sensors, which were monitored by a data-acquisition system that sampled and stored the data every 10 seconds.

Table 2. Surface meteorological sensors.

Sensor	Type	Accuracy	Response
Air temperature (ta)	Platinum RTD	0.1°C	10 s
Sea temperature (ts)	Platinum RTD	0.1°C	30 s
Relative humidity (RH)	Crystallite fiber	6%	60 s
Wind speed (U)	Cup	1%	1.5 m
Wind direction (D)	Vane	1 deg	1.1 m

In operation, measurements were recorded 24 hours per day. To reduce the volume of data, statistics of rms and standard deviation were locally computed at 10-minute intervals. Approximately 60 samples of surface meteorology and approximately 1000 samples of power monitored at the analyzer were used to compute these statistics. The local data (statistics) were automatically transferred for further analysis via modem lines to computers at the Naval Ocean Systems Center, about 10 miles south of the receiver site.

Evaporation duct height and molecular absorption were computed from observed rms values of surface meteorology. Absorption-free path loss was determined by a look-up procedure into a precomputed two-dimensional table. One dimension of this table was evaporation duct height from 0 (standard) to 20 meters in 2-meter intervals; the other dimension was rms bump height specified at 0 (smooth surface), 0.25, and 0.50 meters.

RESULTS

MEASUREMENT PERIODS

Measurements began in late July 1986 and continued through early July 1987. Eight periods, totaling 102 days of operations, were completed during this time. Table 3 lists the time periods in which measurements were made.

Table 3. Dates of measurements.

Start	End
July 29, 1986	August 10
September 2, 1986	September 11
October 7, 1986	October 20
November 18, 1986	November 23
December 1, 1986	December 23
January 13, 1987	January 30
May 4, 1987	May 14
June 30, 1987	July 5

One-way transmission-path data were analyzed by comparing observed rms path loss (transmission loss) to path loss computed for both evaporation duct height and rms bump height, which were calculated from surface meteorological quantities measured at the receiver site. Absorption-free path loss calculated by MLAYER was modified by adding molecular absorption loss calculated from surface meteorology[1] in order to compare it to observed total path loss. Molecular absorption loss during the entire measurement program averaged approximately 30 dB.

Figures 7 through 14 show the time-series of surface meteorology, measured path loss, and predicted path loss for the eight time periods. Measurements and results from each of these time periods are discussed in the following paragraphs.

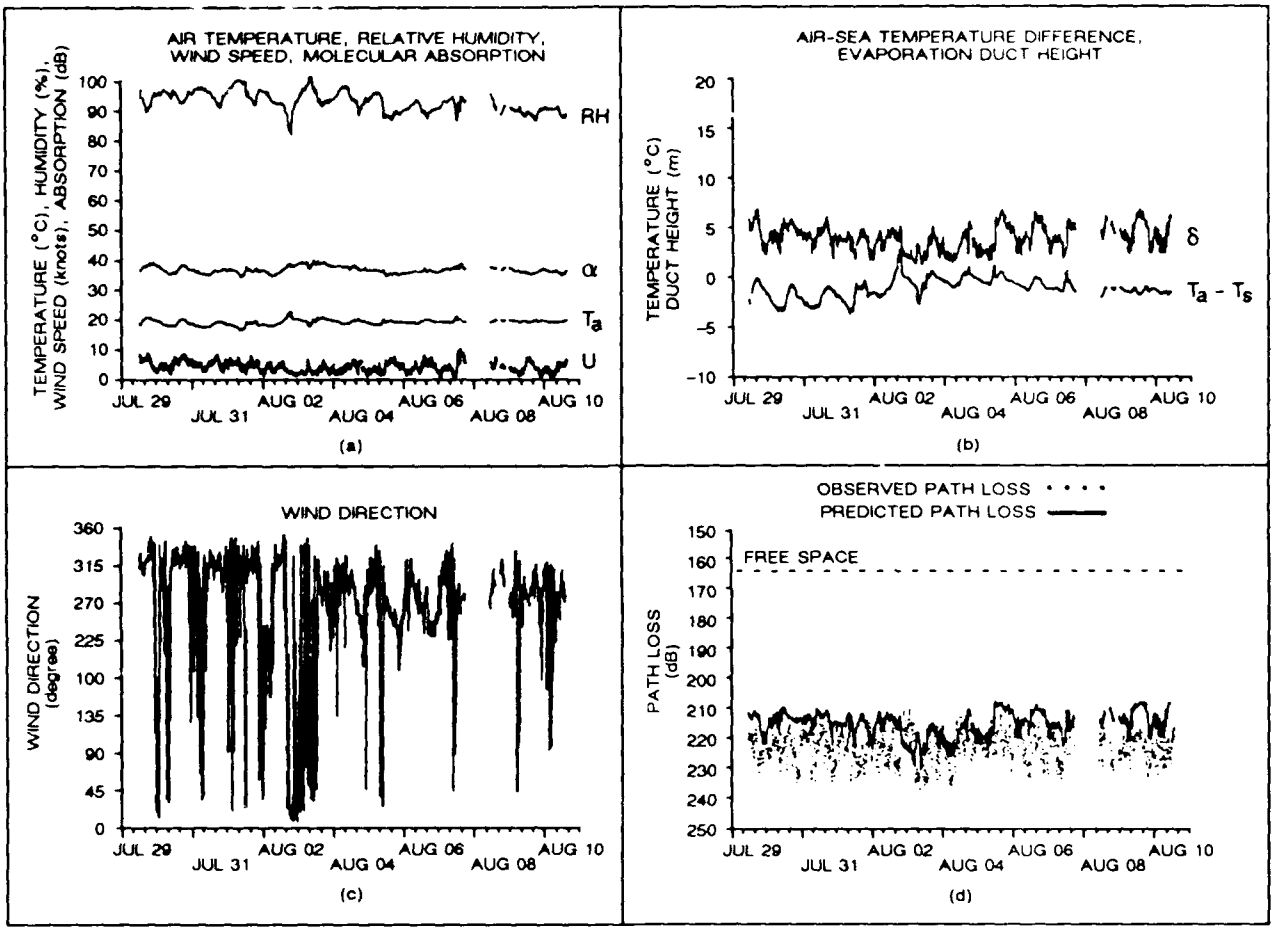

Figure 7. July 29 through August 10, 1986 data.

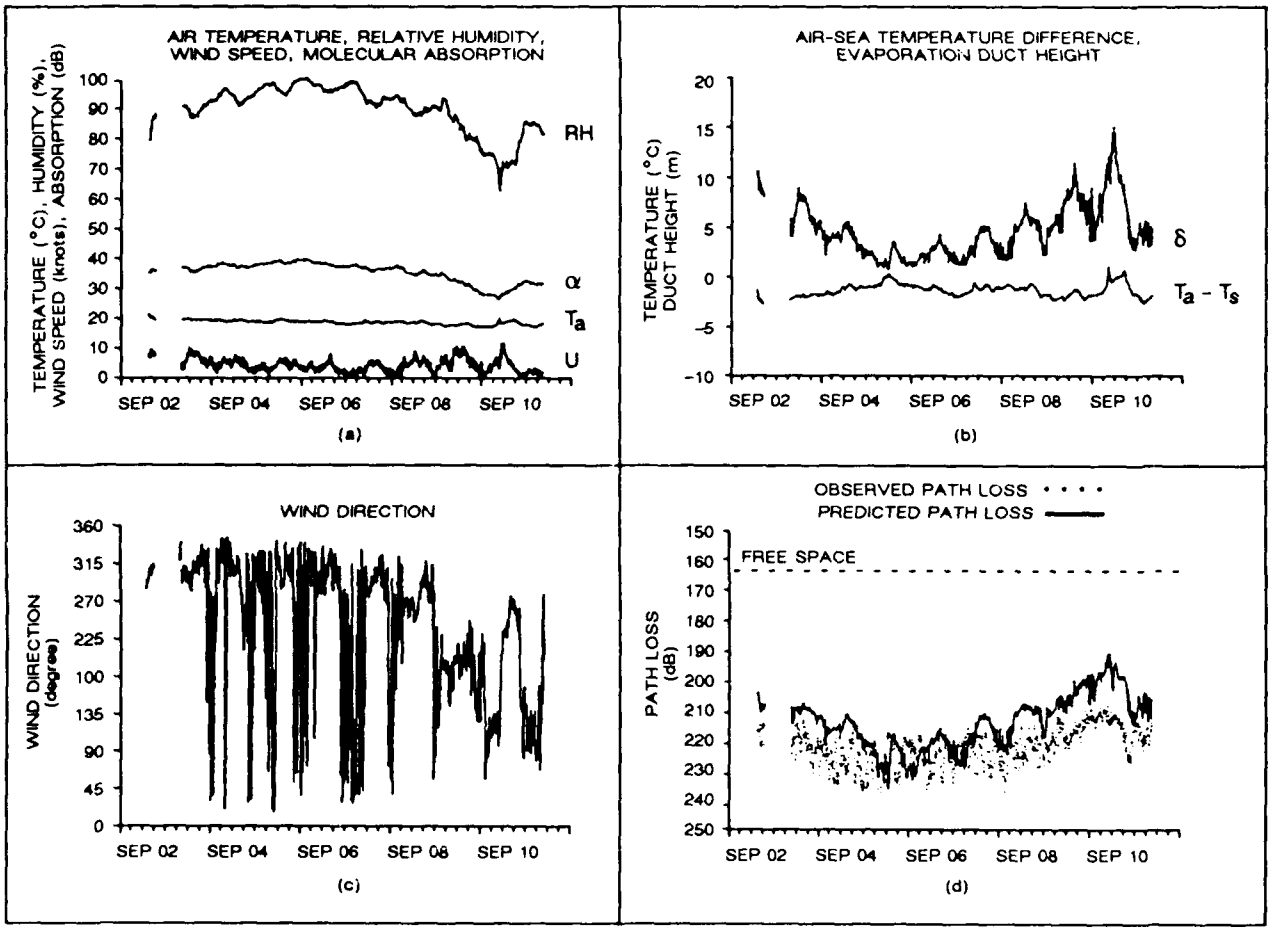

Figure 8. September 2 through September 11, 1986 data.

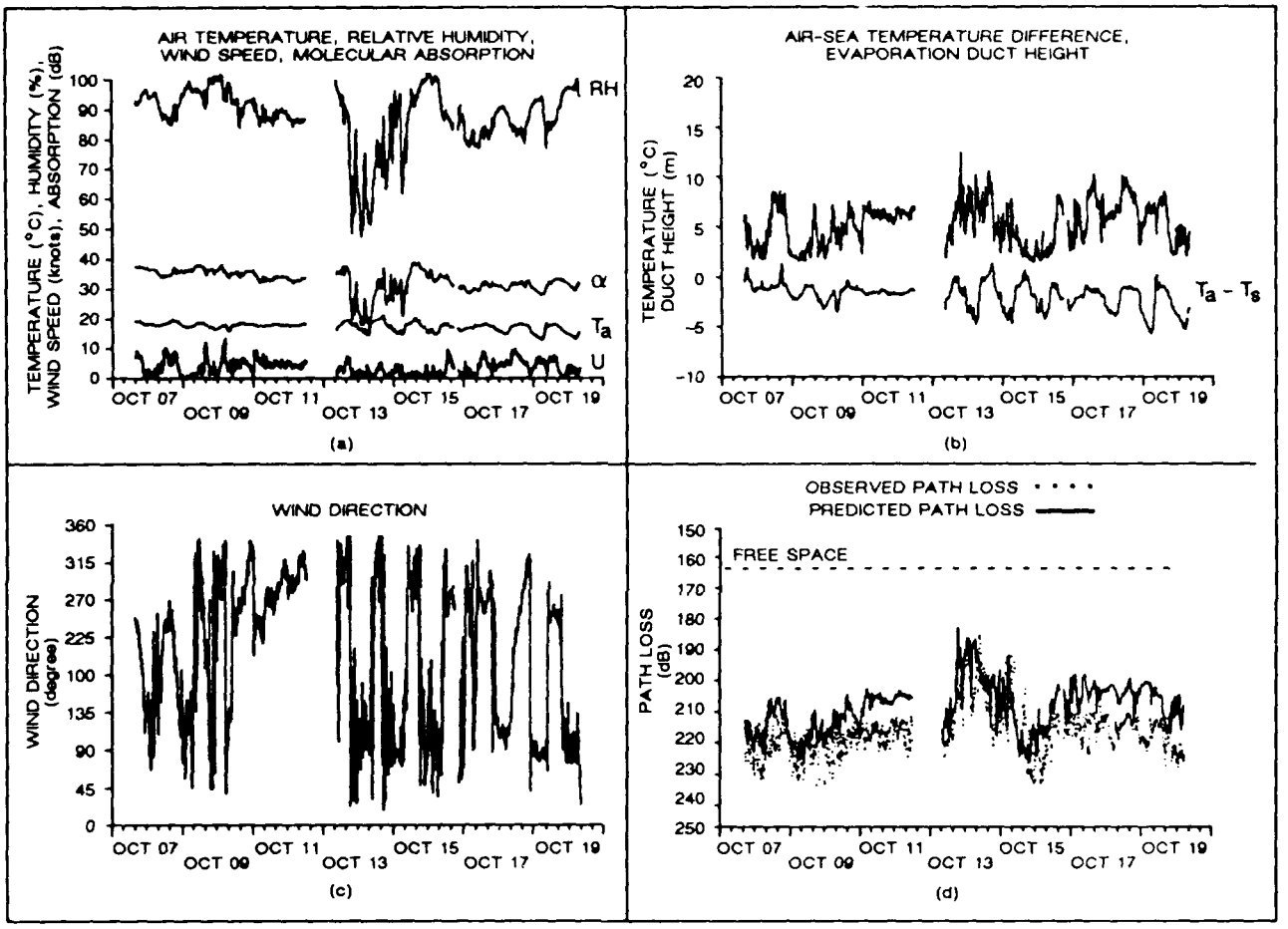

Figure 9. October 7 through October 20, 1986 data.

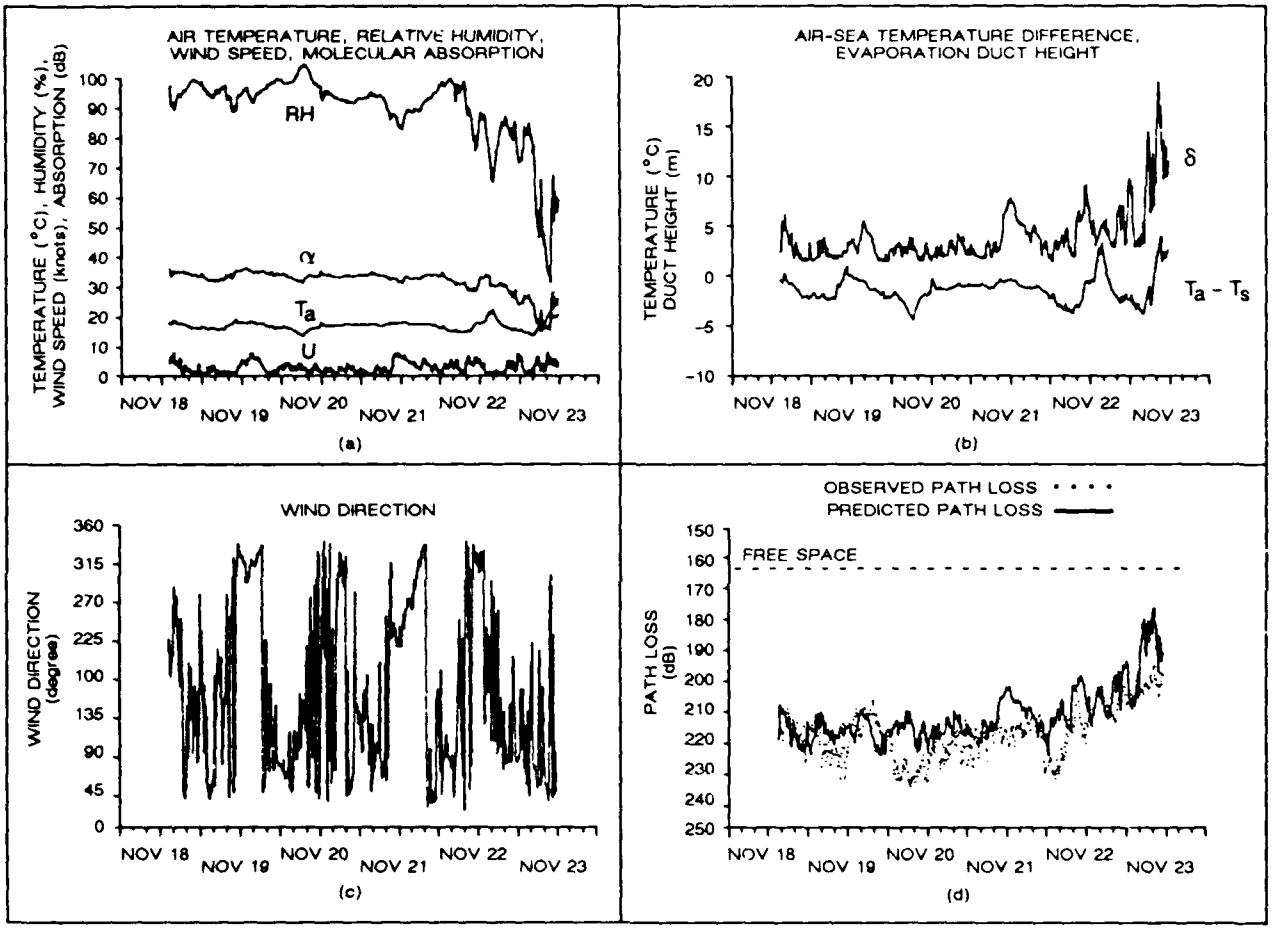

Figure 10. November 18 through November 23, 1986 data.

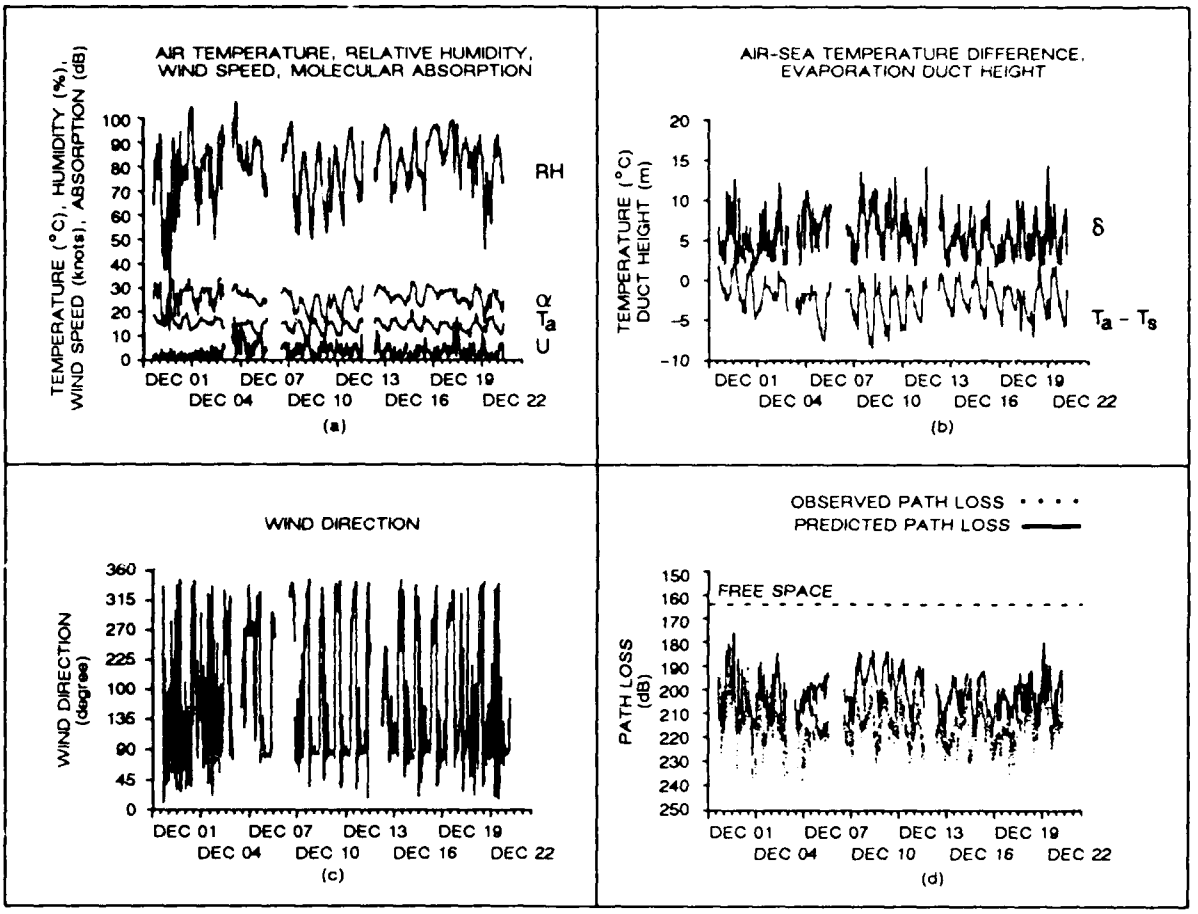

Figure 11. December 1 through December 23, 1986 data.

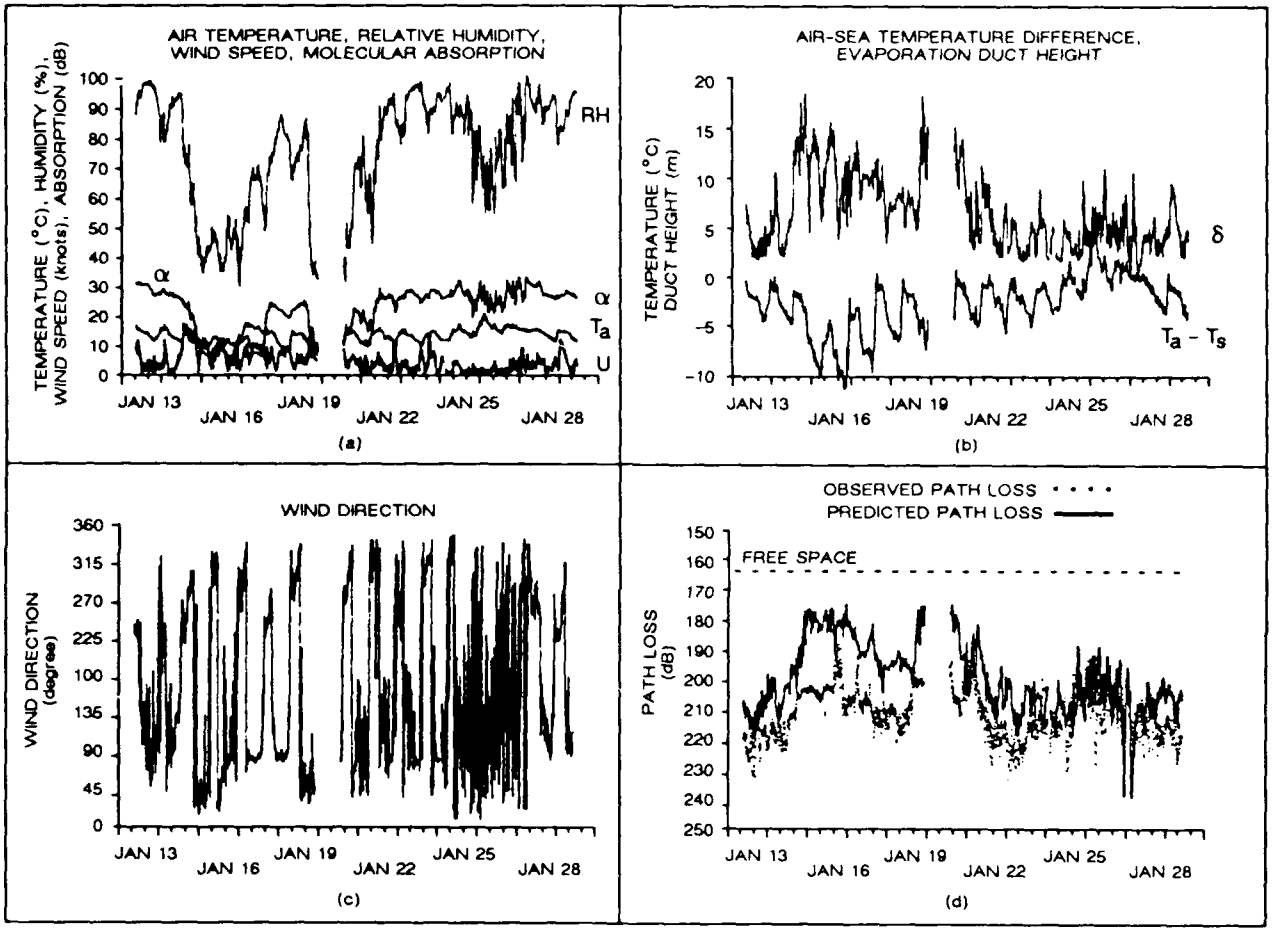

Figure 12. January 13 through January 30, 1987 data.

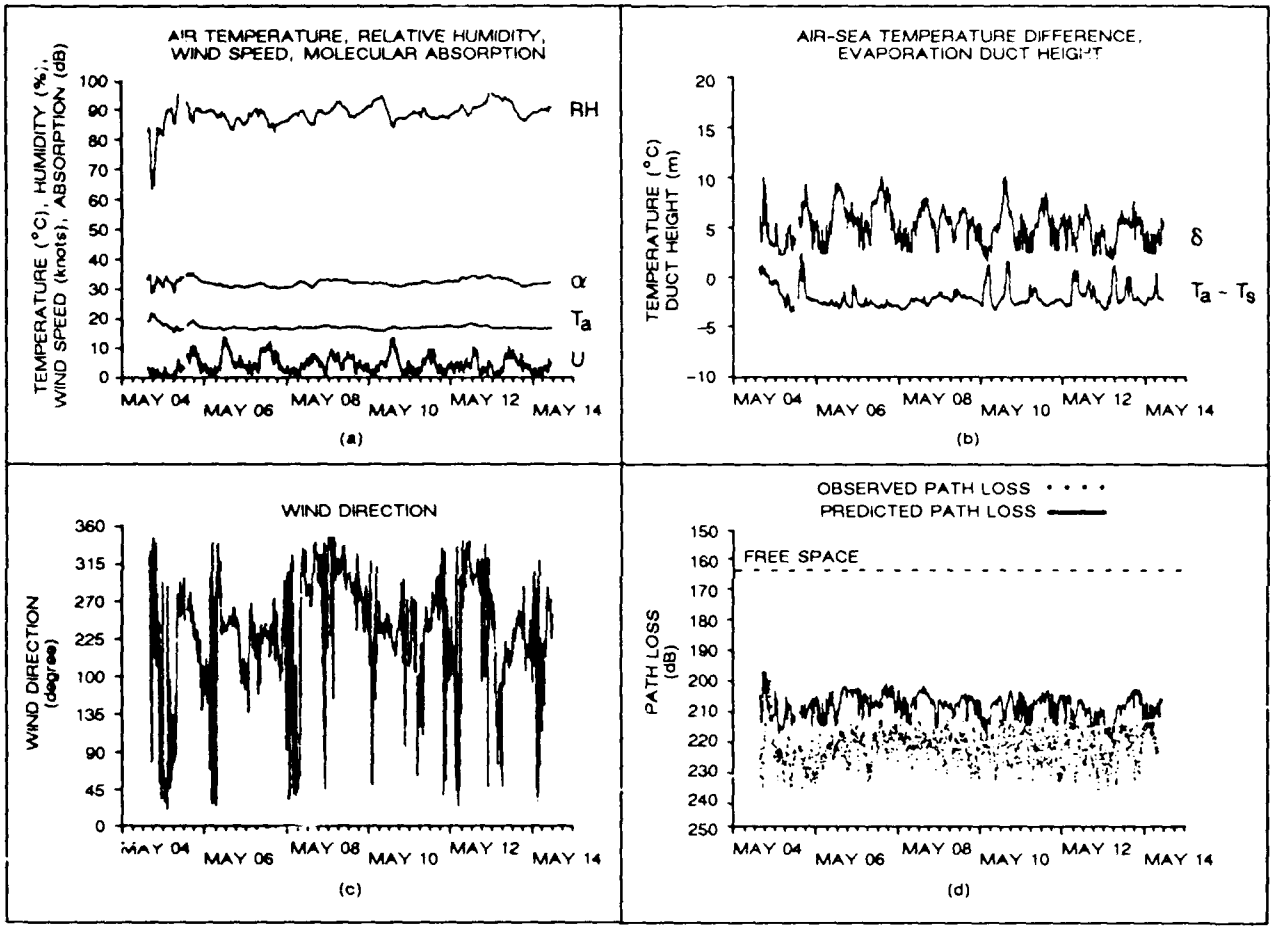

Figure 13. May 2 through May 14, 1987 data.

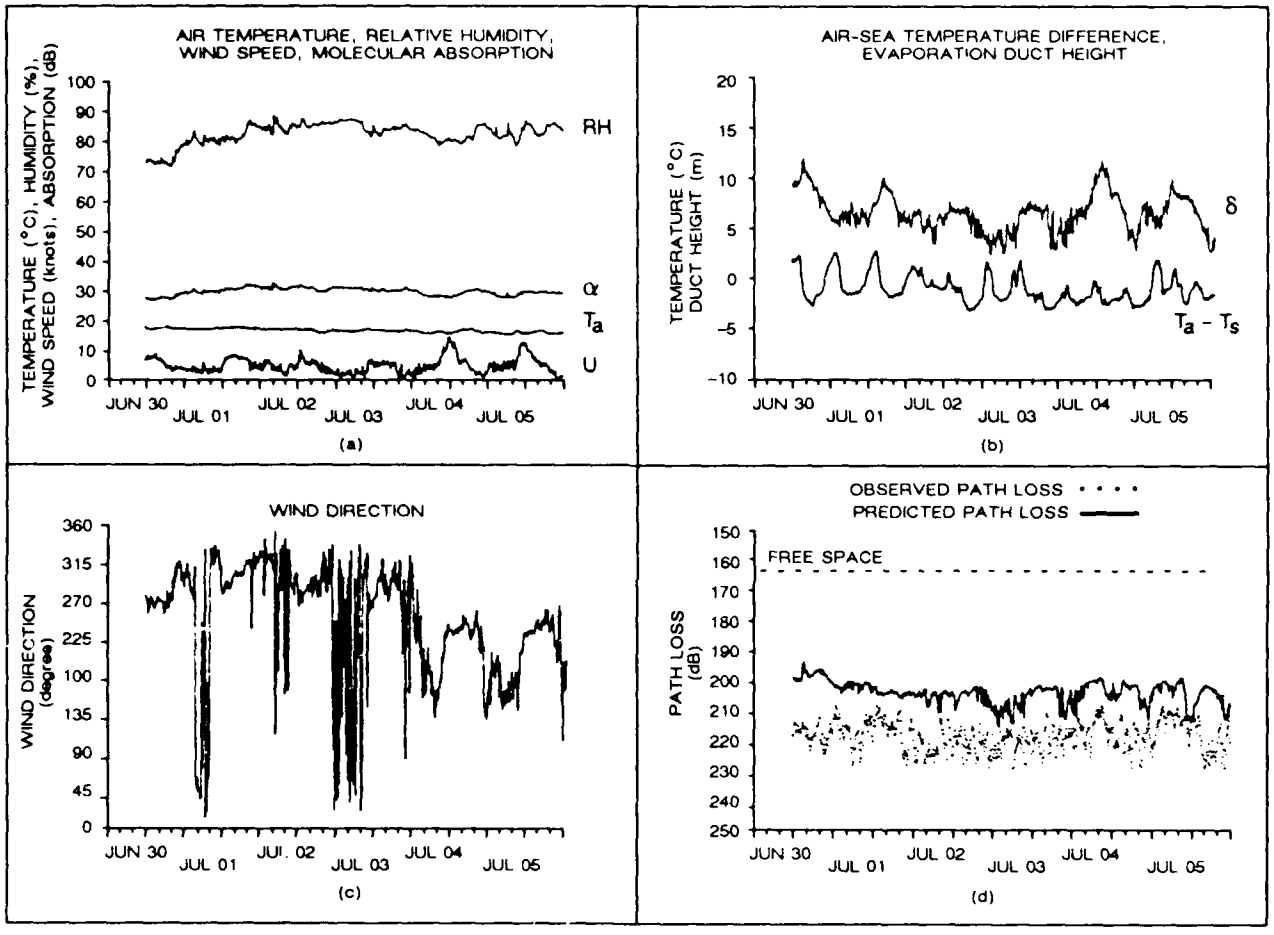

Figure 14. June 30 through July 5, 1987 data.

July 29 through August 10, 1986

Figure 7a is a time-series plot of measured air temperature, relative humidity, and wind speed for the period from July 29 through August 10, 1986. Also included in this figure is the computed molecular absorption, labeled as α. The time shown on the abscissa is plotted in local time; hour 00 is associated with the tic mark above the first character in the date label. A gap in the data around August 8 was due to a software failure that was eventually corrected. This failure caused the data-acquisition system to "hang" and stop collection until manually cleared; data gaps apparent in different time periods are related to other software and hardware failures that had to be manually cleared. In this period, relative humidity was nearly always greater than 90%, accompanied with light winds. Sea temperature was fairly constant at about 20°C. Figure 7b shows the air–sea temperature difference and the calculated evaporation duct height. Diurnal changes of about 3°C in air temperature are observed early in this period and become less pronounced later. Wind direction, Fig. 7c, shows some land–sea breeze effects up until about August 4, when the breeze became fairly constant from the northwest. Figure 7d shows the observed and predicted path loss. Predicted path loss is derived from adding the calculated absorption to the path loss calculated for the evaporation duct height on a point-by-point basis. Considering that the propagation model assumes spatial and temporal homogeneity along the entire 40.6-km path, the time-series agreement between the observed and predicted path loss is remarkable.

With no evaporation ducting, the estimated path loss is the sum of the diffraction path loss and the molecular absorption. The diffraction loss for the path geometry is 250 dB; the average molecular absorption loss is seen to be about 35 dB (Fig. 7a); therefore the estimated path loss with no evaporation ducting is about 285 dB. From Fig. 7d, the average observed path loss is about 225 dB, which is 60 dB less than what is expected if standard or 4/3 earth propagation prediction models were used. However, the observed path loss is about 60 dB greater than the free-space level (164 dB), which means that radar applications are unlikely unless the target has a large radar cross-section.

September 2 through September 11, 1986

The time-series plots for the period of September 2 through September 11, 1986, are presented as Fig. 8a through 8d in the same manner as for the previous period. Wind speed was higher here than for the July–August period, but was mostly less than 10 knots. Both air temperature and sea temperature were relatively constant—diurnal changes in air temperature are not readily observed. Relative humidity gradually decreased from nearly 100% to about 70% from September 7 through September 10; molecular absorption decreased in the same manner. Associated with the decrease in humidity is the change in wind direction from the northwest to almost due east. The difference between the predicted path loss and the observed path loss gradually increases (in this same time period) with the predicted value underestimating the observed (Calculations indicate a higher received power than observed). The differences noted between September 7 and September 10 are probably associated with an incorrect assumption of homogeneity along the path.

October 7 through October 20, 1986

Figures 9a through 9d show results from the October 1986 measurement period. Of particular interest is the period between October 13 and October 15, during which a change in the environment was indicated by a sharp decrease in local relative humidity, a general decrease in wind speed, and larger diurnal changes in air temperature (Figs. 9a and b). Sharp land–sea breeze changes are shown in Fig. 9c. Sea temperature varied slightly in the October period and averaged 19.5°C. Molecular absorption decreased 15 dB, evaporation duct height increased by 5 meters, and path loss decreased by 30 dB, coming within some 25 dB of free-space levels. If the evaporation duct had no effect on signal transmission, one would expect path loss to decrease by the same amount as molecular absorption loss. However, a 15-dB decrease in path loss was predicted for the increased duct height, which accounts for the observation. The good tracking of temporal variation illustrates modeling accuracy and, for at least this period, supports the assumption of horizontal homogeneity.

Errors between prediction and observation (Fig. 9d) are most likely attributable to lack of additional sensors along the path; the assumption of horizontal homogeneity does not always hold. For example, from October 11 to October 12, wind speed (Fig. 9a) was relatively constant, about 2.5 m/s, blowing from southwest to northwest (Fig. 9c) directly from the ocean—seemingly ideal conditions to assess evaporation ducting effects; however, predictions underestimate observation by more than 10 dB. Although wind direction did not switch from a sea breeze to a land breeze (which indicates an atypical mesoscale circulation), additional surface data are not available to explain the discrepancies between prediction and observation.

November 18 through November 23, 1986

The period of November 18 to November 23, 1986, is fairly similar to the October period and is shown in Fig. 10a through 10d. Around November 23, a 20-dB underestimation in predicted path loss is associated with a large decrease in humidity, which is associated with a land breeze. In the early morning hours of November 20 and November 22, a land breeze was present, and the predicted path loss underestimates the observed path loss by about 20 dB. A 15-dB underestimation in path loss, around noon on November 21, is associated with a westerly flow at about 7 knots. The humidity plot (Fig. 10a) indicates 104% on the morning of November 20. The humidity sensor is accurate to 6% which explains the erroneous 104% reading.

December 1 through December 23, 1986

The striking feature of the data shown in Fig. 11a through 11d are the substantial diurnal variations in humidity, air temperature, and wind direction. From December 10 through December 15, predicted path loss is consistently 10 to 15 dB less than the observed path loss; however, the tracking of signal fluctuations is remarkable. The tracking of the signal power gives strong support to the usefulness of the propagation model even though the model appears to be biased toward underestimation.

January 13 through January 30, 1987

Figures 12a through 12d show the data for the period of January 13 through January 30, 1987. From early morning on January 15 through the evening hours of the same day, the humidity rapidly decreased from 90% to 35%, wind speed changed from calm to 15 knots, and wind direction changed from nearly due east to nearly due west. On this day, the predicted path loss underestimates the observed path loss by up to 30 dB. The relatively calm period from January 25 through January 28 is when the predicted path loss closely matches the observed path loss. The indications that the largest disagreement between predicted and observed path loss is associated with high winds and that the best agreement between predicted and observed path loss is associated with low wind speeds lead to a speculation that the formulation of surface roughness in the propagation model is lacking.

May 4 through May 14, 1987

A feature of Fig. 13a through 13d is the presence of a fog bank situated several hundred meters westward and along the propagation path. This fog bank, though not recorded in the measurements, is noted in the manual log entries. Liebe et al. report that the absorption rate can increase by 0.5 dB/km in the presence of fog.[1] If this additional absorption were added to the calculated molecular absorption, the predicted path loss would increase about 20 dB, bringing it into close agreement with the observed path loss.

June 30 through July 5, 1987

The period of June 30 through July 5, 1987, shown in Fig. 14a through 14d, is similar to the May period in that the predicted path loss is consistently 20 dB less than the observed path loss; however, there was no observed fog bank as in the May period. Although the reason for the underestimation is unknown, the most likely source for the error is the assumption of spatial and temporal homogeneity.

ALL MEASUREMENT PERIODS COMBINED

The crucial parameter that relates path loss to surface meteorological conditions is evaporation duct height. A scatter plot of difference between observed and predicted path loss in relation to calculated duct height is shown in Fig. 15. All 102 days of observations, more than 12,000 data points, are included. Predicted path loss, on average, underestimates observed path loss by approximately 10 dB and, in the extremes, underestimates by nearly 40 dB and overestimates by 22 dB. A trend line, computed from a histogram of scatter, indicates median error. The trend is for error to increase with duct height up to heights of about 5 meters; median error is relatively flat for higher duct heights.

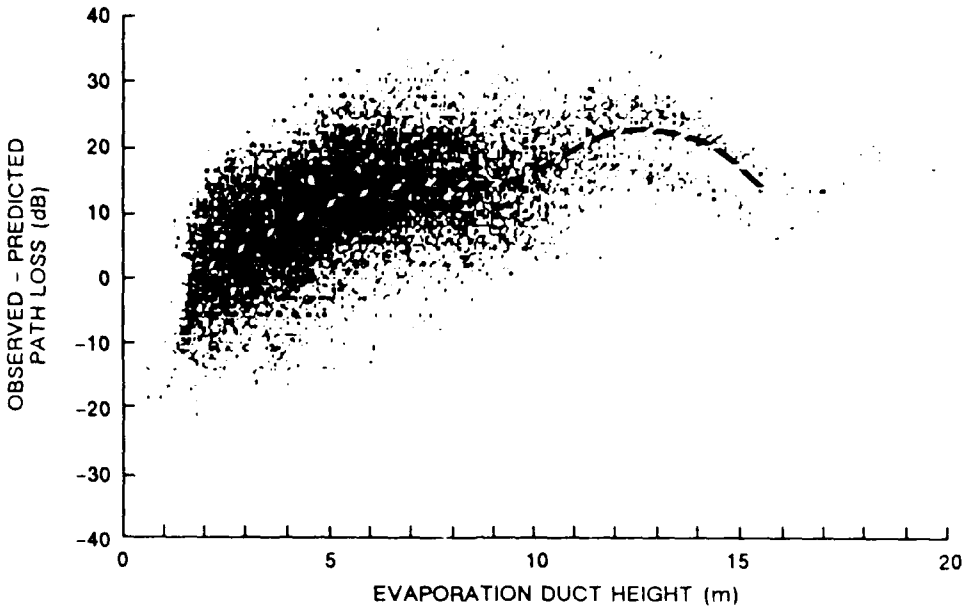

Figure 15. Error between predicted and observed path loss in relation to observed evaporation duct height. All data measured, without qualification, are presented. A positive error indicates prediction underestimates observation.

Wind speed strongly affects both evaporation duct height and surface roughness. Higher winds generally increase duct height and increase attenuation due to roughness. A scatter plot of error in path loss with relation to wind speed is shown in Fig. 16. A trend line indicates that median error is about 2.5 dB for winds less than 1 knot and increases to 14 dB at about 5 knots. For winds greater than about 5 knots, error remains nearly constant at about 14 dB. It is tempting to reduce the error bias by modifying rms bump height, because the surface roughness formulation in MLAYER is one of the largest uncertainties at millimeter wavelengths. However, the measurement program was designed to test for gross environmental effects; a modification to rms bump height or surface roughness formulation cannot be justified from these data.

An interesting relationship between observed relative humidity and path loss error is shown by the scatter plot in Fig. 17. A trend line through the scatter indicates that error is greater at lower humidities than it is at higher humidities; reasons for this trend are not clearly understood. This same trend is also observed in scatter plots of air–sea temperature difference and molecular absorption; the latter is expected because absorption is a strong function of humidity. Correlations between humidity and wind speed, wind direction, and air temperature are weak and provide no additional insight. A correlation of humidity and duct height is also weak.

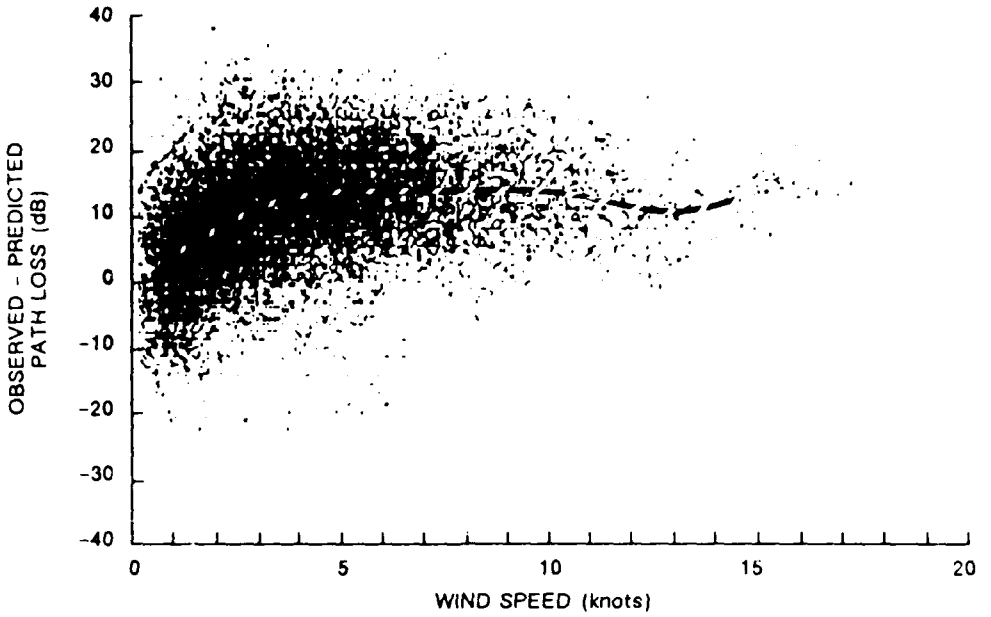

Figure 16. Path loss error in terms of observed wind speed for all measurements.

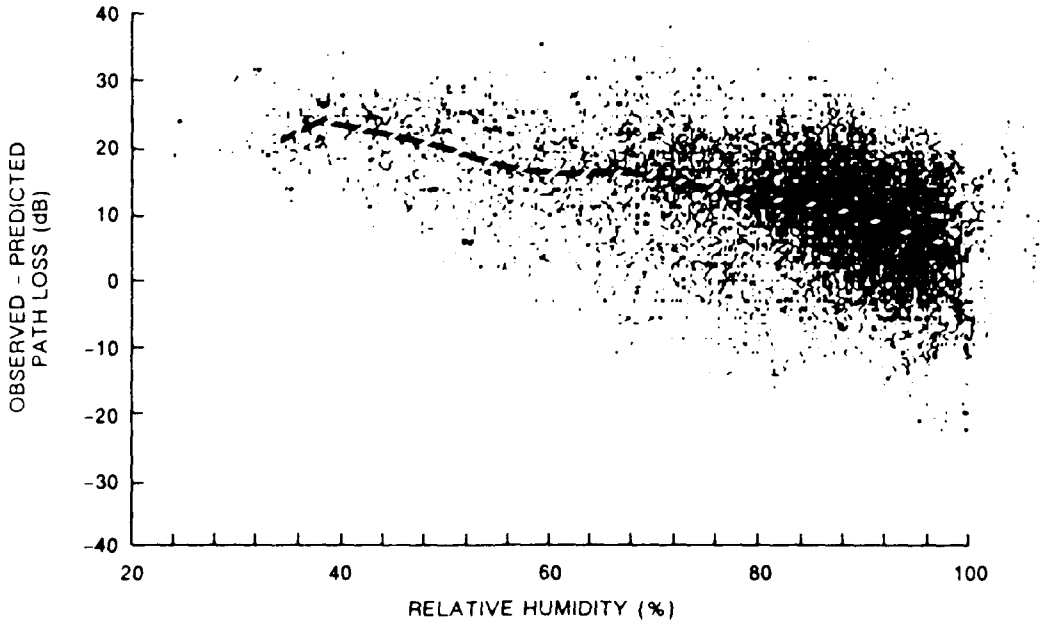

Figure 17. Path loss error in terms of observed relative humidity for all measurements. Why error increases for decreasing humidity is not understood.

CLIMATOLOGY

A comparison of observed absorption-free path loss to predictions derived from a separate climatology of evaporation duct heights[7] illustrates an application of the propagation model to the assessment of a millimeter-wave system. The evaporation duct climatology is based on 15 years of surface meteorological observations (normally taken by ships at sea) from which the distribution of evaporation duct heights were computed. All ocean areas were analyzed in 10-degree × 10-degree grids (Marsden squares). For the San Diego offshore area (Fig. 18), the frequency distribution shows a peak for duct heights between 6 and 10 meters. Duct heights greater than 20 meters are infrequent. Combining this distribution with the results shown in Fig. 3 (0.25-meter bump height) gives an accumulated frequency distribution which is shown as a solid line in Fig. 19. Observed absorption-free path loss is plotted on the same figure as a dotted line. Free-space and diffraction fields are referenced. Although the predicted path-loss distribution consistently underestimates the observed path loss, it is clearly a better predictor than could be attained by assuming a standard atmosphere representation of the environment. In the worst case, it is only some 10 dB less than the observed path loss, whereas the difference is about 4 dB at the 50% level. The observed path loss reduction from diffraction exceeds 63 dB half of the time; 90% of the time the reduction exceeds 55 dB. Both predicted and observed distributions show that path loss is 45 dB less than the diffraction reference 100% of the time (the occurrence of rain was negligible during the measurements).

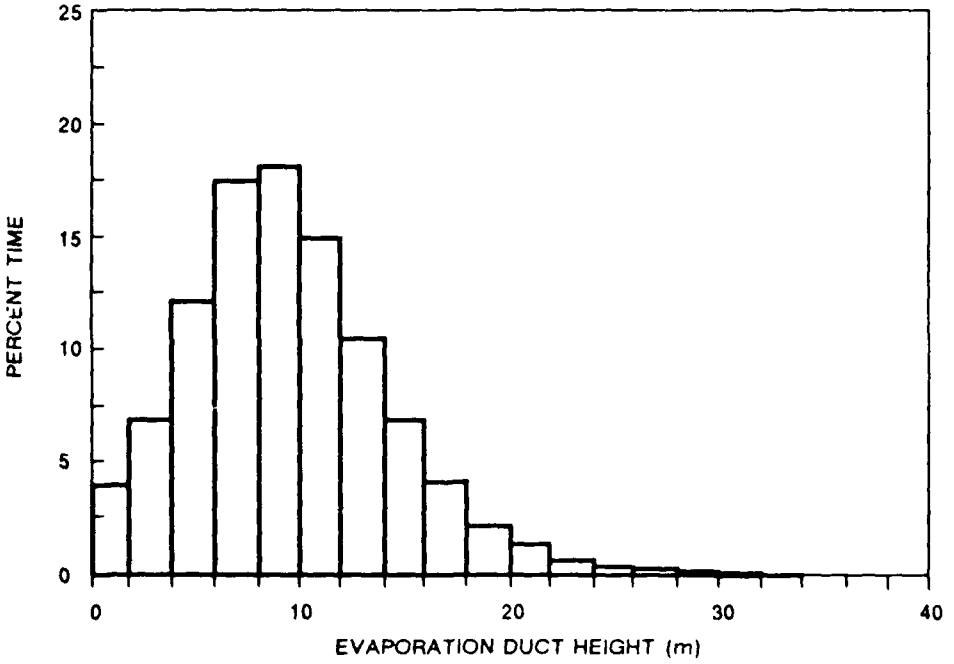

Figure 18. Climatological evaporation duct height distribution for the San Diego offshore area.

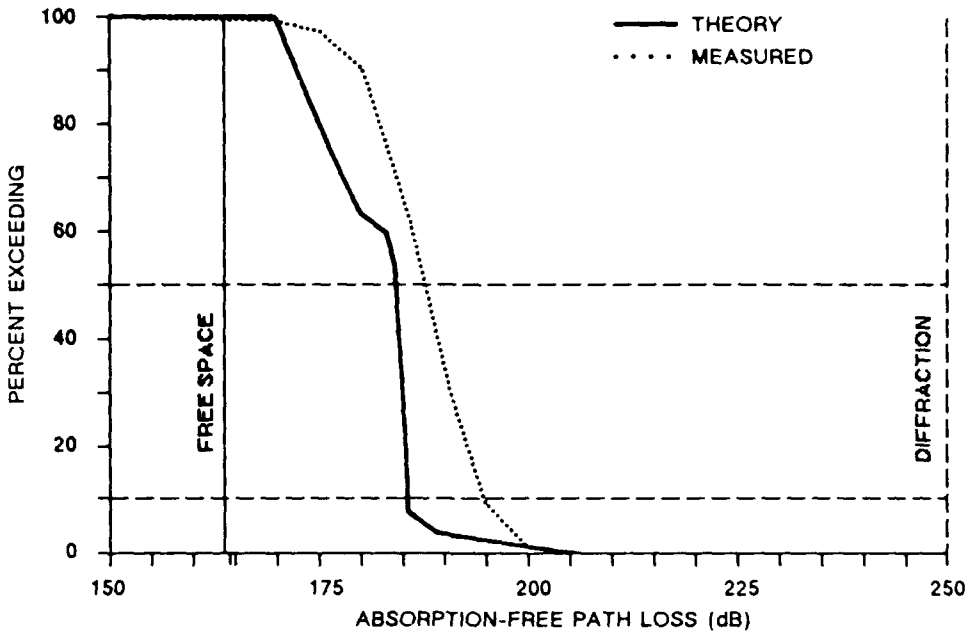

Figure 19. Absorption-free path loss distribution predicted from the distribution in Figure 13 compared to the measured path loss. Total path loss can be approximated by reading the desired percentage and adding 30 dB (average absorption loss) to the corresponding abscissa coordinate.

CONCLUSIONS

The low-altitude propagation of millimeter waves at ranges beyond the radio horizon is strongly influenced by the evaporation duct; for the propagation path used, received power levels are 50 to 100 dB greater than the power levels expected for propagation through a nonducting standard atmosphere.

A single-station measurement of surface meteorology is adequate to analyze millimeter-wave propagation over the ocean. On a point-by-point comparison, modeling typically underestimates observations by about 10 dB; the error is probably due to incomplete considerations of both horizontal heterogeneity and surface roughness effects. The direct sensing of the environment on the scale of kilometers in the horizontal and meters in the vertical is impractical, however, planetary boundary layer models and remote sensing techniques may, in the future, offer considerable improvement to the propagation analysis. The formulation of surface roughness in the propagation model is actively being examined for a more complete understanding.

In summary, the increase in received signal strength resulting from the presence of the evaporation duct has been realistically modeled and provides an accurate estimate of actual millimeter-wave system performance. The significant system "gain" due to evaporation ducting is clearly an important consideration in the design stages of moderate-range, over-water millimeter-wave systems.

REFERENCES

1. H.J. Liebe, K.C. Allen, G.R. Hand, R.H. Espeland, and E.J. Violette, "Millimeter-wave propagation in moist air: model versus path data," NTIA Report 85-171, 54 pp., March 1985.

2. R.K. Crane, "Fundamental limitation caused by RF propagation," Proc. IEEE, vol. 69, pp. 196-209, 1981.

3. M. Katzin, R.W. Bauchman, and W. Binnian, "3- and 9-centimeter propagation in low ocean ducts," Proc. IRE, vol. 35, pp. 891-905, September 1947.

4. H. Jeske, "Die Ausbreitung elektromagnetischer Wellen im cm- bis m-Band uber dem Meer unter besonderer Berucksichtigung der meteorologischen Bedingungen in der maritimen Grenzschicht," Hamburger Geophys. Einzelschriften, Hamburg, DeGruyter and Co., 1965.

5. J.H. Richter and H.V. Hitney, "Antenna heights for the optimum utilization of the oceanic evaporation duct," Naval Ocean Systems Center TD 1209, 513 pp., January 1988.

6. K.D. Anderson, "Evaporation duct effects on moderate range propagation over the sea at 10 and 1.7 cm wavelengths," Naval Ocean Systems Center TR 858, November 1982.

7. W.L. Patterson, "Climatology of marine atmospheric refractive effects," Naval Ocean Systems Center TD 573, 523 pp., December 1986.

8. H. Jeske, "State and limits of prediction methods of radar wave propagation conditions over sea," paper presented at the NATO Advanced Study Institute, Sorrento, Italy, 5–14 June 1973.

9. H.V. Hitney, "Propagation modeling in the evaporation duct," Naval Electronics Laboratory Center TR 1947, 38 pp., April 1975.

10. R.A. Paulus, "Practical application of an evaporation duct model," Radio Sci., vol. 20, pp. 887-896, 1985.

11. H.V. Hitney, J.H. Richter, R.A. Pappert, K.D. Anderson, and G.B. Baumgartner, Jr., "Tropospheric radio propagation assessment," Proc. IEEE, vol. 73, pp. 265-283, 1985.

12. H. Jeske, "The state of radar-range prediction over sea," Tropospheric Radio Wave Propagation Part II, AGARD, pp. 50-1,50-6, February 1971.

13. H.G. Booker and W. Walkinshaw, "The mode theory of tropospheric refraction and its relation to waveguides and diffraction," in Meteorological Factors in Radio Wave Propagation. London, England: The Physical Society, 1946, pp. 80-127.

14. K.G. Budden, *The Waveguide Mode Theory of Wave Propagation*, London,England: Logos Press, 1961.

15. L.M. Brekhovskikh, *Waves in Layered Media*, 2nd ed. New York: Pergamon, 1970.

16. G.B. Baumgartner, Jr., "XWVG: A waveguide program for trilinear tropospheric ducts," Naval Ocean Systems Center TD 610, 206 pp., June 1983.

17. D.G. Morfitt and C.H. Shellman, "'MODESRCH', an improved computer program for obtaining ELF/VLF/LF mode constants in an earth atmosphere waveguide," Interim Rep. 77T, prepared for the Defense Nuclear Agency by the Naval Electronics Laboratory Center (now Naval Ocean Systems Center), 227 pp., October 1976.

18. W.D. Ament, "Toward a theory of reflection by a rough surface," Proc. IRE, vol. 41, pp. 142–146, 1953.

19. O.M. Phillips, *Dynamics of the Upper Ocean*, London: Cambridge Univ. Press, 1966.